Mechanic and Energy

Characterization of the soot generated by an internal combustion engine using blends of biodiesel through Raman spectroscopy

Maysa Teixeira Resende[1,5]

https://orcid.org/0000-0002-7775-9280

Júlio César Costa Campos[2,6]

https://orcid.org/0000-0002-9488-8164

Luciano de Moura Guimarães[3,7]

https://orcid.org/0000-0001-9656-2996

Joaquim Bonfim Santos Mendes[3,8]

https://orcid.org/0000-0001-9381-0448

José Antônio Silva[1,9]

https://orcid.org/0000-0003-4813-1029

Antonio Marcos de Oliveira Siqueira[4,10]

https://orcid.org/0000-0001-9334-0394

Gustavo Rodrigues de Souza[1,11]

https://orcid.org/0000-0002-7461-2152

[1]Universidade Federal de São João Del-Rei - UFSJ, Departamento de Ciências Térmicas e dos Fluídos, Programa de Pós-graduação em Engenharia de Energia, São João Del-Rei – Minas Gerais - Brasil.

[2]Universidade Federal de Viçosa - UFV, Departamento de Engenharia de Produção e Mecânica, Viçosa - Minas Gerais – Brasil.

[3]Universidade Federal de Viçosa - UFV, Departamento de Física, Viçosa - Minas Gerais – Brasil.

[4]Universidade Federal de Viçosa - UFV, Departamento de Química, Viçosa - Minas Gerais – Brasil.

E-mails: [5]mteixeiraresende@gmail.com, [6]julio.campos@ufv.br, [7]lucianomoura@ufv.br, [8]joaquim.mendes@ufv.br, [9]jant@ufsj.edu.br, [10]antonio.siqueira@ufv.br, [11]souzagr@ufsj.edu.br

Abstract

Biodiesel serves as a biodegradable, non-toxic, and renewable fuel option that offers an alternative to traditional fossil fuels. This study aimed to examine the impact of elevating biodiesel content to 20% and 50% within regular diesel, with a focus on comprehending how these fuel mixtures influence variations in soot composition using Raman spectroscopy. The soot samples under analysis originated from commercial S10 diesel, as well as fuel blends containing 20% and 50% portions of sunflower and macaúba biodiesel, whereupon the use of this methodology for these fuels characterizes the novelty of this work. The outcomes derived from analyzing the soot samples revealed distinct characteristics in the G, D1, D3, and D4 bands. The ratio between the intensities of these D and G bands is closely indicative of the soot's structure. Consequently, this ratio was analyzed in this investigation to assess the effects of biodiesel concentration and engine rotation speed on soot characteristics. The conclusions found in this study indicated that there was minimal variation in the spectral characteristics of the soot samples across the different fuels and varying engine speeds. As a result, it is inferred that increasing the proportion of biodiesel in commercial diesel S10 did not have a significant impact on the structural composition of soot.

Keywords: soot, Raman spectroscopy, blends of biodiesel, diesel.

1. Introduction

The continued growth of energy demand, depletion of fossil fuel reserves and awareness of environmental issues have encouraged the development of research on renewable energy sources. In this scenario, biodiesel is an attractive alternative fuel for diesel engines. Biodiesel is biodegradable, renewable, non-toxic and is also safe for transport and storage (Liu *et al.*, 2011; Miranda *et al.*, 2014; Hilário *et al.*, 2024). It is the only commercially available renewable alternative to diesel fuel, and it offers the potential of both reducing fossil carbon emissions and producing alternative clean transportation fuels (Boehman, Juhun Song and Alam, 2005; Vander Wal *et al.*, 2007). Biodiesel is produced from the transesterification of vegetable oils, seaweed and animal fat (Hilário *et al.*, 2024). It is compatible with the diesel engine's structure, and it can be mixed in various proportions with conventional fuel, or it can be used directly in engines without further modifications. Comparative experiments demonstrated that the diesel and biodiesel have similar burning characteristics and power (Bi, Qiao and Lee, 2013; Can, 2014; Lapuerta, Armas & Rodríguez-Fernández, 2008; Xiao *et al.*, 2014).

Engines fueled with biodiesel can reduce carbon monoxide (CO), total hydrocarbons (THC), and particulate materials (Lapuerta, Armas, and Rodríguez-Fernández, 2008). Some studies have reported that biodiesel is responsible for a slight increase in nitrogen oxide (NOx) emissions, but that can be solved through advanced engine techniques, such as optimized injection and exhaust gas recirculation (EGR) (Bi, Qiao, and Lee, 2013; George *et al.*, 2007; Jing *et al.*, 2015; Lapuerta, Rodríguez-Fernández, and Oliva, 2012; Shihong Yan *et al.*, 2005; Yoon, Suh, and Lee, 2009; Silva *et al.*, 2023).

Among environmental pollutants emitted by diesel engines, soot has become a major concern because of its impact on the environment and human health (Lépicier, Chiron, and Joumard, 2013). The soot nuclei having radii between 0.1 and 0.5 µm can be deposited in the lungs, resulting in serious health problems (Antusch *et al.*, 2010; Kim *et al.*, 2011; Xiao *et al.*, 2014). Soot is related to engine performance and emission characteristics. Therefore, the real effect that soot particulate has in the engines has been of interest to research (Vander Wal & Tomasek, 2004). Different engine load conditions and alternative fuel formulations can produce differences in morphology and in the nanostructure of the soot (Fang & Lee, 2009). Previous studies have shown that due to the oxygen content ~10% (by weight) in biodiesel soot emissions decreases regularly as biodiesel concentration increases in a blend of fuels (Fang *et al.*, 2008, 2009; Wang *et al.*, 2012). Therefore, it is possible that a change in fuel composition reduces particle emissions in a diesel engine.

Soot can be defined as the product of incomplete combustion or pyrolysis of fossil fuels and other organic materials (Sadezky *et al.*, 2005). Soot from diesel burning is mainly composed of carbon (> 80%), but also by hydrogen, oxygen, nitrogen and sulfur (Esangbedo, Boehman, and Perez, 2012). In soot, carbon has different states of hybridizations.

The structure of soot is characterized by an agglomeration in the form of chains which may reach hundreds of nanometers in size. The soot agglomerates are known as secondary particles of soot and are formed of spherical or nearly spherical units known as primary soot particles. The primary soot particles may contain from 105 to 106 carbon atoms and their size can vary from 15 to 50 nm (Friedrich, 2012).

The carbon atoms in the primary soot particles are arranged in platelets, or an array of face-centered hexagonals, while multiple layers of platelets form crystals (Friedrich, 2012). The average distance between the platelets is 0.355 nm, that is, slightly different of the characteristic graphite distance (0.335 nm) (I. Glassman, 1996).

The physical-chemical structure of the soot, as well as its elemental composition and the proportion of graphitic structures compared to amorphous carbon depend on a variety of factors including the fuel used and the conditions of pyrolysis or combustion (Sadezky *et al.*, 2005).

Raman spectroscopy is widely used in the study of carbonaceous materials. Among the advantages of this technique, there can be mentioned the necessity of a minimum quantity of samples, which do not need to be pre-treated. Raman spectroscopy is sensitive to the different arrangements of the carbon atoms and can reveal the structure and intrinsic defects in the network. The intensity, the width and the position of the characteristic bands of the carbon material spectrums are dependent on the extent of the material graphitization (Esangbedo, Boehman, and Perez, 2012; Mather *et al.*, 2007; Seong & Boehman, 2013). Moreover, Raman spectroscopy is an important technique in the study of carbonaceous materials, such as soot. This technique presents a high sensitivity to crystallinity, hybridization, and chemical-physical interaction between materials (Li *et al.*, 2023).

In previous studies, Boehman *et al.* (2005) showed that the nanostructure and oxidation reactivity of the primary soot particles are modified by biodiesel fueling. The aim of this article is to correlate the influence of fuels with different proportions of biodiesel and diesel in the soot structure using Raman Spectroscopy and in the characteristic curves of the engine.

Other studies evaluated the influence of the addition of some polycyclic aromatic hydrocarbons in a mixture with diesel, showing emission rates (De Albuquerque *et al.*, 2013; Yilmaz *et al.*, 2023; Yilmaz; Davis, 2022; Yilmaz & Donaldson, 2022; Yilmaz; Rafiei and Donaldson, 2023; Yilmaz; Vigil and Donaldson, 2022, 2023).

Therefore, Raman spectroscopy has been used in several researches related to the study of soot, and this research aimed to verify the differences generated in soot, for mixtures of biodiesel, macaúba and sunflower, which are rarely available in literature, with proportions of 20% and 50% and using this methodology.

2. Materials and methods

2.1 Experiment
2.1.1 Diesel Engine and fuels

This study was conducted in a four-stroke diesel engine model TD200 and manufactured by Hatz Diesel. This engine has a single cylinder with a stroke of 62 mm, a crankshaft radius of 31 mm, engine displacement of 232 cm³, compression ratio 22:1, and stroke/diameter ratio equal to 1. Five types of blends in volume fuels were analyzed: conventional diesel (S10), a blend of 20% sunflower biodiesel with the conventional diesel (BS20), a blend

of 50% sunflower biodiesel with the commercial diesel (BS50), a blend of 20% macaúba biodiesel with the commercial diesel (BM20) and a blend of 50% macaúba biodiesel with the commercial diesel (BM50). Mechanical stirring was carried out until the mixture reached phase homogeneity, and then

left to rest for 72 hours, without phase separation being noticed.

The biodiesel was produced by the transesterification method. This method could be better used for biodiesel production, and it has the purpose of decreasing the viscosity of vegetable or animal oils. Potassium hydroxide (KOH) was the

catalyst, and anhydrous methanol was the transesterification agent. The quality of biodiesel is specified based on various physical-chemical characteristics of the fuel, which directly influence (Hilário *et al*., 2024).. Therefore, Table 1 presents the physical-chemical characteristics of the fuels in study.

Table 1 - Physical-chemical characteristics of the fuels analyzed.

Fuel	Density (kg/m³)	Kinematic Viscosity (x 10⁻⁶ m²/s)	Flash point (°C)	LHV (MJ/kg)
S10	830 ±1	3.99 ±1.2%	61.8 ±0.1	44.0 ±5.0%
BM	888 ±1	5.62 ±1.2%	109.0 ±0.1	39.3 ±5.0%
BM20	850 ±1	4.27 ±1.2%	79.5 ±0.1	43.1 ±5.0%
BM50	865 ±1	5.34 ±1.2%	85.6 ±0.1	42.0 ±5.0%
BS	860 ±1	5.30 ±1.2%	135.6 ±0.1	42.0 ±5.0%
BS20	842 ±1	4.49 ±1.2%	82.4 ±0.1	43.9 ±5.0%
BS50	857 ±1	5.16 ±1.2%	104.7 ±0.1	43.5 ±5.0%

Source: Authors.

The density in Table 1 shows the relationship between the mass and the volume at a specified temperature, which in Brazil is 20 °C. Values outside of the specified range indicate the presence of contaminants. Limiting the density range is important for the design of the injection system and for the operation of the engine. The kinematic viscosity in Table 1

represents the flow time of a fluid through a capillary tube with standardized dimensions, under the action of the force of gravity, while the flash point consists of the lower temperature at which the emission of flammable vapors by diesel begins.

The engine tests were performed under full load. To obtain the engine parameters, seven different engine speeds were analyzed.

The characteristic curves of the engine were obtained using the VDAS software.

The soot produced from the fuels was obtained at low (1800 rpm) and high rotation (3000 rpm) of the engine. The soot particles were extracted from the exhaust gas stream by direct deposition in microscopy glass slides for posterior analysis in EDX and Raman Spectroscopy (Figure 1).
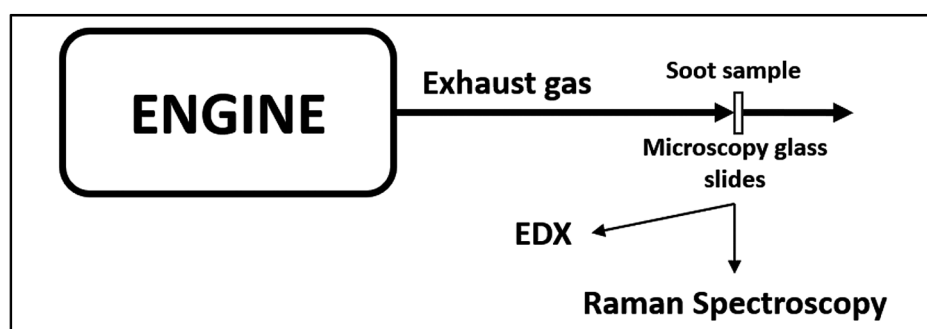
Figure 1 - Schematic view of test facility.

2.1.2 The energy dispersive x-ray (EDX)
The EDX measurements were realized with a field emission scanning electron microscope Model JEOL-6010LA.

2.1.3 Raman spectroscopy
Raman scattering spectra were obtained by a Micro Raman spectrometer in-Via Renishaw. The Raman measurements

were performed at three different points for each soot sample using a 50x objective. The measurements were performed with

the 514.5 nm laser line of an Ar laser and power around 1 mW. The spot laser size on the samples was around 1µm of diameter.

3. Results and discussion

3.1 EDX analysis
Energy Dispersive X-ray Spectroscopy (EDX) is an analytical method that leverages the fluorescence phenomenon of a material when subjected to a beam of electrons or X-rays. This technique

is commonly employed for elemental analysis or chemical characterization of a given sample. Figure 2 shows the energy dispersive X-ray (EDX) analysis of a typical sample of soot resulting from the com-

bustion of sunflower biodiesel. The EDX spectrum taken from an arbitrary region in the sample shows only the presence of carbon (C) and oxygen (O). The additional peak of the silicon (Si) in the spectrum is

due to the glass support on which the soot samples are deposited for analysis. For the case of diesel, the presence of carbon and oxygen as the combustion product was also verified. For all samples, the results show that the product of the combustion of diesel and biodiesel is composed mainly of carbon (over 99%) with a small percentage of oxygen (below 1%).
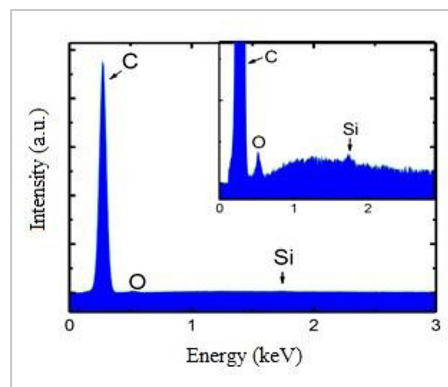
Figure 2 - The energy dispersive X-ray (EDX) spectra of soot obtained from the combustion of sunflower biodiesel.

The EDX spectrum detailing the position of the peaks of the oxygen and silicon is shown in the insert.

3.2 Raman spectroscopy analysis

Raman spectroscopy is an important technique in the study of carbonaceous materials, such as soot. This technique presents high sensitivity to crystallinity, hybridization, and chemical-physical interaction between materials (Li *et al.*, 2023). In this study, soot spectra were investigated to evaluate the influence of fuel on the structural variations of diesel exhaust soot. The standard spectrum of soot has two main bands: a band known as a D band with around 1360 cm^{-1}, associated with structural disorder of sp^2 bonds, and a band known as the G band (graphite band) with around 1580 cm^{-1} (Xiao *et al.*, 2014).

In order to acquire detailed information about the soot particles structures, it is essential to deconvolute (curve-fit) the Raman spectra (Li, Hayashi, and Li, 2006). For the analysis, OriginPro 8.6 and Peak fit v4.12 software were used. The deconvoluted spectra were obtained with the adjustment method that got the best statistical results. Some researchers, among them Sadezky *et al.* (2005), Seong & Boehman (2013), and Sheng (2007) consider that the combination of Lorentzian in D1, D4 and G bands with a Gaussian in D3 band can get the best fit for the spectrum soot. However, there is still no clear consensus among researchers about the most suitable fitting for the spectra of amorphized carbonaceous materials and the establishment of a reliable and reproducible method (Li, Hayashi, and Li, 2006). In this study, the spectra were deconvoluted by Voigt curve fit, which achieved the best statistical parameters, such as the coefficient of determination R^2.

The Voigt function can be defined as the convolution of the Lorentzian and Gaussian distribution functions. The Gaussian distribution is also known as the normal distribution function. This function is traditionally recognized as a tool for modeling multi-causal phenomena, due to the central limit theorem results. The Lorentzian distribution is also known as the Cauchy distribution function. This distribution is mainly found in spectroscopy and is sometimes referred to as the natural shape of a spectral line. The effects that give rise to a Gaussian line shape tend to be independent of giving rise to a Lorentzian form. Therefore, the convolution of these two types of functions results in the theoretical model to a spectral line when both types of amplification are present (Sheng, 2007).

The spectra of all soot samples in study were deconvoluted by Voight resulting in four bands: D1 with 1357 cm^{-1}, D3 with 1526 cm^{-1}, D4 with 1178 cm^{-1} and the G band at 1598 cm^{-1}. Figure 3 shows the Raman spectrum of BS20 at high rotation (3000 rpm) deconvoluted by Voight.
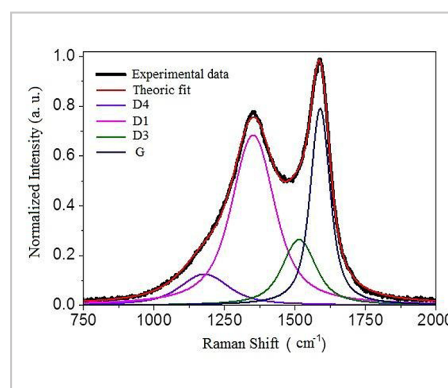
Figure 3 - Experimental Raman data fitted by four Voight curves.

The G-band at 1598 cm^{-1} is shown in blue in the figure and it is the main feature of the spectra of graphitic materials. This band is associated with tangential vibration in the plane of carbon atoms in sp^2 bonds (Gołąbczak & Konstantynowicz, 2009; Kouketsu *et al.*, 2014; Patel *et al.*, 2012).

The D1 band at 1357 cm^{-1} is associated with structural disorder in sp^2 carbonate systems and is indicated in pink in the figure. In graphene / graphite, this band is the result of the breaking of the hexagonal symmetry of the network by heteroatoms, edges, or network faults (Patel *et al.*, 2012). The relationship between the peaks D1 and G (ID1/IG) can be used to correlate the structures of the carbon materials, enabling the quantitative analysis of the degree of disorder in the material (Dixon Dikio, 2011; Lépicier,

Chiron, and Joumard, 2013; Russo & Ciajolo, 2015; Sadezky *et al.*, 2005; Seong & Boehman, 2013; Vander Wal *et al.*, 2007; Zaida *et al.*, 2007).

The D3 band in 1526 cm^{-1} is indicated in green in Figure 3. This band has its origin related to the amorphous sp^2 carbon fraction of the soot (Gołąbczak & Konstantynowicz, 2009).

The D4 band at 1178 cm^{-1} is shown in purple in Figure 3. This band appears only in amorphous materials, such as soot and coal. Its origin can be attributed to sp^3 structures disordered or ionic impurities (Li, Hayashi, and Li, 2006).

After adjustment and deconvolution of the spectrum in Figure 3, it can be noted that no band was observed at 1620 cm^{-1}. This band could be called D2 in the present context and is known as

D' in the graphene spectrum. This result was reproduced for all fuel soot samples under study. The D2 band also occurs due to the disorder in the graphitic structure (Minutolo *et al.*, 2011). Previous studies have reported the difficulties in separating the G and D2 bands by fitting (Dixon Dikio, 2011; Li, Hayashi, and Li , 2006; Seong & Boehman, 2013). However, in an amorphous carbon system, it is not expected to find a D' band, since this band originates from a second-order process in the k point for the graphene Brillouin zone (Malard *et al.*, 2009).

The ratios ID1/IG, ID3/IG and ID4/IG were calculated after the spectral deconvolution for each fuel studied for the engine at high (3000 rpm) and low rotation (1800 rpm) and the results are shown in Table 2.

Table 2 - Ratio of the intensities of the bands D and G for fuels analysis for high and low rotation.

	I(D1/IG)		I(D3/IG)		I(D4/IG)	
	HR	LR	HR	LR	HR	LR
S10	0.90 ±0.05	0.95 ±0.02	0.39 ±0.06	0.38 ±0.02	0.16 ±0.02	0.18 ±0.00
BS20	0.87 ±0.02	0.93 ±0.02	0.34 ±0.02	0.36 ±0.01	0.16 ±0.00	0.18 ±0.00
BS50	0.90 ±0.03	0.94 ±0.06	0.35 ±0.04	0.37 ±0.04	0.15 ±0.02	0.17 ±0.02
BM20	0.93 ±0.05	0.94 ±0.04	0.40 ±0.04	0.41 ±0.03	0.17 ±0.02	0.18 ±0.01
BM50	0.91 ±0.02	0.98 ±0.02	0.40 ±0.02	0.40 ±0.01	0.16 ±0.01	0.17 ±0.01

Source: Authors.

Figure 4 illustrates the ratio of intensities between the D1 and G bands (ID1/IG) for soot samples generated from fuel combustion. The graph was developed from the Table 2 data, and it was built with the y axis from 0.8 to 1 to evidence the differences between the samples.
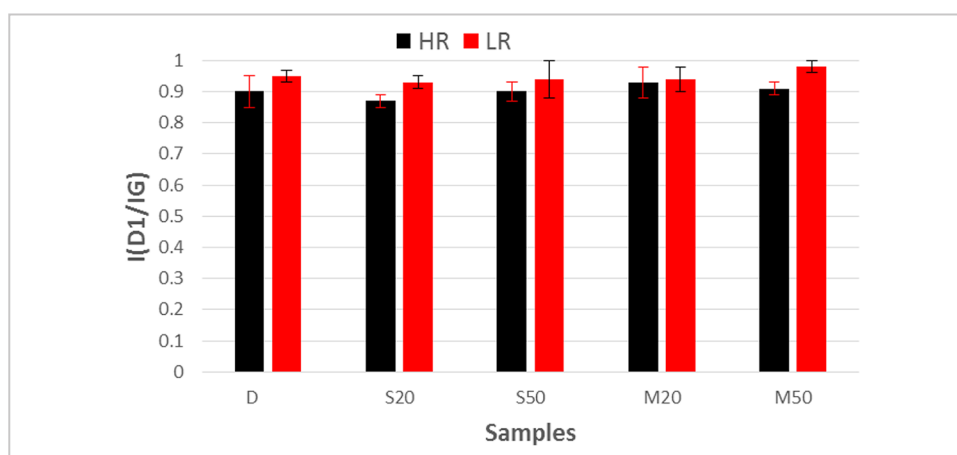
Figure 4 - Graph of the intensity's ratio between D1 and G bands (ID1 / IG) for soot samples from the combustion of fuels in the study.

The Figure 4 analysis indicates that the ratio of the intensities of the bands D1 and G, ID1/IG show slightly larger values for samples collected at low speed (1800 rpm) than for the samples collected at high speed (3000 rpm. This trend is replicated for all fuels under study. The ID1/IG ratio is directly proportional to the degree of disorder of the material structure. The higher ID1/IG greater will be the disorder of the chain.

Therefore, it can be inferred that when the diesel engine runs at low speed, about 1800 rpm, it will produce soot with a more disorganized structure than when the engine is running at high speed, approximately 3000 rpm.

The graph of Figure 4 also suggests

a difference between the fuels with sunflower biodiesel ratios, and with macaúba biodiesel proportions. Regardless of the percentage of biodiesel in the fuel, it can be noted that fuels containing macaúba biodiesel presented the ID1/IG ratio greater than the fuels with sunflower biodiesel proportions. This result remained at both high (3000 rpm) and at low speed (1800 rpm). It can be concluded that the raw material for biodiesel influences the soot chain structure, but

this tendency must be confirmed with more research using other raw materials (Lindner *et al.*, 2015).

Regarding the proportion of biodiesel added to the fuel, the graph of Figure 4 indicates that there were some fluctuations among the values of the ID1/IG ratio for soot samples from diesel fuels with 20% of biodiesel and fuels containing 50% of biodiesel. However, the graph does not show any strong trend among values ID1/IG and the proportion of biodiesel in the fuel. The

graph results suggest that an increase in the proportion of biodiesel in the commercial diesel does not significantly affect the clutter of the soot chain structure.

Figure 5 represents the graph of the ratio between the intensities of the bands D3 and G, ID3/IG, for soot samples from the combustion of fuels in analysis. This graph was developed from the Table 2 data and its y-axis varies between 0.3 and 0.42 to highlight the differences between the results of the samples.
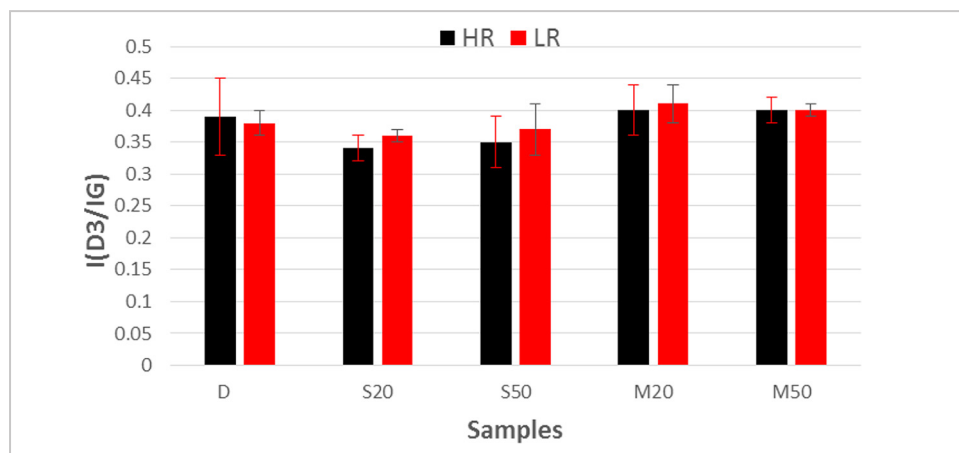
Figure 5 - Graph of the intensity's ratio between D3 and
G bands (ID3/IG) for soot samples from the combustion of fuels in the study.

The analysis of the graph of Figure 5 indicates that fuels containing macaúba biodiesel percentages showed the highest values for the intensity's ratio of the bands D3 and G, ID3/IG. This result was reproduced for both low speed (1800 rpm) and for high speed (3000 rpm). The ratio ID3/IG is related to the presence of amorphous carbon soot. Higher values of ID3/IG indicate higher concentrations of amorphous carbon. Therefore, the graph results suggest that the raw material of biodiesel can influence the soot structure. According to the data, fuels with macaúba

biodiesel ratios showed a soot with a higher concentration of amorphous carbon.

The graph in Figure 5 indicates that the conventional diesel showed higher values for the ID3/IG ratio at high speed than at low speed. While the fuels BG20, BG50 and BM20 presented values for the ID3/IG ratio lower at high speed than the values at low speed. Finally, the BM50 fuel had almost the same value of ID3/IG ratio both at high and at low speed. The ID3/IG ratio is related to the concentration of the amorphous carbon material. Higher values of ID3/IG indicate higher

concentrations of amorphous carbon. The soot samples studied showed small variations in relation to this ratio, and they did not show any strong trend. Therefore, the results obtained by the ID3/ IG ratio indicate that a higher concentration of biodiesel, as well as the engine speed, does not affect the structure of soot compared to amorphous carbon.

Figure 6 shows the graph that represents the intensity ratio of the bands D4 and G, ID4/IG, for soot samples from the combustion of the fuels studied.
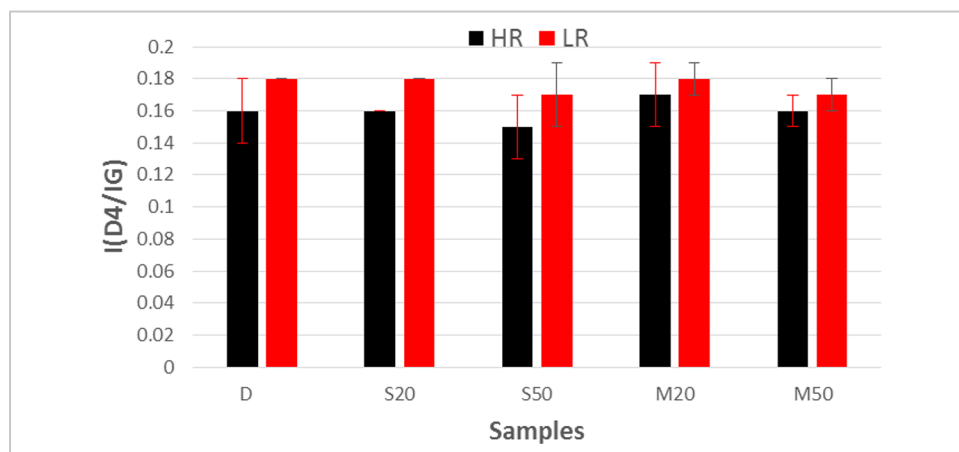
Figure 6 - Graph of the intensity's ratio between D4 and
G bands (ID4/IG) for soot samples from the combustion of fuels in the study.

The graph in Figure 6 shows that the soot samples presented slightly higher results for the ratio of bands D4 and G, ID4/IG at low speed (1800 rpm) compared to values at high speed (3000 rpm). This trend is reproduced for soot samples from all the investigated fuels.

The analysis of Figure 6 also indicates that the ID4/IG ratio showed no significant differences between the soot samples. Therefore, through the graph data, it can be concluded that an increase in the concentration of biodiesel in diesel fuel, as well as the type of biodiesel, does not affect the ID4/IG ratio of the soot samples.

It is important to highlight that, as these are oilseeds typical of Brazil, no similar studies were found for comparisons with the mixtures studied.

4. Conclusions

Raman spectroscopy is a promising technique in the study of carbonaceous materials, but it still faces some challenges for the study of highly disordered materials, such as soot. To establish the best fit and decomposition for the soot spectrum is the major concern for the reliability of this technique.

Currently, the prevailing Brazilian law, since April 2023, ensures a 12% incorporation of biodiesel in commercial diesel. Based only in the results obtained with the physical and chemical analysis of fuel soot in this study, Brazilian legislation could increase biodiesel concentration to 20% in commercial diesel.

This study aimed to examine the impact of elevating biodiesel content to 20% and 50% within regular diesel, with a focus on comprehending how these fuel mixtures influence variations in soot composition, using Raman spectroscopy. Our results suggest that the composition of soot is independent of the type of diesel used. EDX analyses reveal that the carbon to oxygen ratio in soot is not affected by mixing. Furthermore, evaluations by Raman spectroscopy indicate that soot is predominantly composed of amorphous carbon, whose structure does not present significant variations between different samples and is not influenced by the engine rotation regime.

In future studies, a more detailed analysis of the morphology (with a Scanning Electron Microscopy) of the soot should be carried out to identify the differences in the mixtures studied.

Acknowledgments

References

ANTUSCH, Steffen; DIENWIEBEL, Martin; NOLD, Eberhard; ALBERS, Peter; SPICHER, Ulrich; SCHERGE, Matthias. On the tribochemical action of engine soot. *Wear,* v. 269, n. 1-2, p. 1-12, 2010. DOI: https://doi.org/10.1016/j.wear.2010.02.028

BI, Xiaojie; QIAO, Xinqi; LEE, Chia-fon F. Investigation about temperature effects on soot mechanisms using a phenomenological soot model of real biodiesel. *Energy & Fuels,* v. 27, n. 9, p. 5320-5331, 2013. DOI: https://doi.org/10.1021/ef401208b

BOEHMAN, André L.; JUHUN SONG, And; ALAM, Mahabubul. Impact of biodiesel blending on diesel soot and the regeneration of particulate filters. 2005. DOI: https://doi.org/10.1021/ef0500585

CAN, Özer. Combustion characteristics, performance and exhaust emissions of a diesel engine fueled with a waste cooking oil biodiesel mixture. *Energy Conversion and Management,* v. 87, p. 676-686, 2014. DOI: https://doi.org/10.1016/j.enconman.2014.07.066

DE ALBUQUERQUE, José Eduardo; SANTIAGO, Bruno C. L.; CAMPOS, Júlio César C.; REIS, Alexandre M.; DA SILVA, Charles L.; MARTINS, João Paulo; COIMBRA, Jane S. R. Photoacoustic spectroscopy as an approach to assess chemical modifications in edible Oils. *Journal of the Brazilian Chemical Society,* v. 24, n. 3, p. 369-374, 2013. DOI: https://doi.org/10.5935/0103-5053.20130047

DIXON DIKIO, Ezekiel. Morphological characterization of soot from the atmospheric combustion of diesel fuel. *Int. J. Electrochem. Sci,* v. 6, p. 2214-2222, 2011.

ESANGBEDO, Christine; BOEHMAN, André L.; PEREZ, Joseph M. Characteristics of diesel engine soot that lead to excessive oil thickening. *Tribology International,* v. 47, p. 194-203, 2012. DOI: https://doi.org/10.1016/j.triboint.2011.11.003

FANG, Tiegang; LEE, Chia-Fon F. Bio-diesel effects on combustion processes in an HSDI diesel engine using advanced injection strategies. *Proceedings of the Combustion Institute,* v. 32, n. 2, p. 2785-2792, 2009. DOI: https://doi.org/10.1016/j.proci.2008.07.031

FANG, Tiegang; LIN, Yuan-Chung; FOONG, Tien Mun; LEE, Chia-Fon. Reducing NO_x emissions from a biodiesel-fueled engine by use of low-temperature combustion. *Environmental Science & Technology,* v. 42, n. 23, p. 8865-8870, 2008. DOI: https://doi.org/10.1021/es8001635

FANG, Tiegang; LIN, Yuan-Chung; FOONG, Tien Mun; LEE, Chia-Fon. Biodiesel combustion in an optical HSDI diesel engine under low load premixed combustion conditions. *Fuel,* v. 88, n. 11, p. 2154-2162, 2009.

DOI: https://doi.org/10.1016/j.fuel.2009.02.033

FRIEDRICH, A. *Characterization of soot particles from diesel engines and tin dioxide particles milled in stirred media mills.* 2012. Erlangen-Nürnberg University, 2012.

GEORGE, Sam; BALLA, Santhosh; GAUTAM, Vishaal; GAUTAM, Mridul. Effect of diesel soot on lubricant oil viscosity. *Tribology International,* v. 40, n. 5, p. 809-818, 2007. DOI: https://doi.org/10.1016/j.triboint.2006.08.002

GOŁĄBCZAK, M.; KONSTANTYNOWICZ, A. Raman spectra evaluation of the carbon layers with voigt profile materials. 2009.

HILÁRIO, C. V.; CAMPOS, J. C. C.; SIQUEIRA, A. M. de O.; LEITE, M. de O.; MARTINS, M. A.; BRITO, R. F.; ABDERRAHMANE, K. Physical-Chemical properties of first-generation biofuel aiming application in diesel locomotives. *Revista de Gestão Social e Ambiental,* v. 18, n. 5, p. 1-21, 2024. DOI: https://doi.org/10.24857/rgsa.v18n5-042

I. GLASSMAN. *Combustion.* 1996.

JING, Wei; WU, Zengyang; ZHANG, Weibo; FANG, Tiegang. Measurements of soot temperature and KL factor for spray combustion of biomass derived renewable fuels. *Energy,* v. 91, p. 758-771, 2015. DOI: https://doi.org/10.1016/j.energy.2015.08.069

KIM, Kyung Hwan; SEKIGUCHI, Kazuhiko; KUDO, Shinji; SAKAMOTO, Kazuhiko. Characteristics of atmospheric elemental carbon (char and soot) in ultrafine and fine particles in a roadside environment, Japan. *Aerosol and Air Quality Research,* v. 11, p. 1-12, 2011. DOI: https://doi.org/10.4209/aaqr.2010.07.0061

KOUKETSU, Yui; MIZUKAMI, Tomoyuki; MORI, Hiroshi; ENDO, Shunsuke; AOYA, Mutsuki; HARA, Hidetoshi; NAKAMURA, Daisuke; WALLIS, Simon. A new approach to develop the Raman carbonaceous material geothermometer for low-grade metamorphism using peak width. *Island Arc,* v. 23, n. 1, p. 33-50, 2014. DOI: https://doi.org/10.1111/iar.12057

LAPUERTA, Magín; ARMAS, Octavio; RODRÍGUEZ-FERNÁNDEZ, José. Effect of biodiesel fuels on diesel engine emissions. *Progress in Energy and Combustion Science,* v. 34, n. 2, p. 198-223, 2008. DOI: https://doi.org/10.1016/j.pecs.2007.07.001

LAPUERTA, Magín; RODRÍGUEZ-FERNÁNDEZ, José; OLIVA, Fermín. Effect of soot accumulation in a diesel particle filter on the combustion process and gaseous emissions. *Energy,* v. 47, n. 1, p. 543-552, 2012. DOI: https://doi.org/10.1016/j.energy.2012.09.054

LÉPICIER, Véronique; CHIRON, Mireille; JOUMARD, Robert. Developing an indicator for the chronic health impact of traffic-related pollutant emissions. *Environmental Impact Assessment Review,* v. 38, p. 35-43, 2013. DOI: https://doi.org/10.1016/j.eiar.2012.05.001

LI, Xiaojiang; HAYASHI, Jun-Ichiro; LI, Chun-Zhu. FT-Raman spectroscopic study of the evolution of char structure during the pyrolysis of a Victorian brown coal. *Fuel,* v. 85, n. 12-13, p. 1700–1707, 2006. DOI: https://doi.org/10.1016/j.fuel.2006.03.008

LI, Zheling; DENG, Libo; KINLOCH, Ian A.; YOUNG, Robert J. *Raman spectroscopy of carbon materials and their composites*: Graphene, nanotubes and fibers. Progress in Materials Science Elsevier Ltd, 2023. DOI: https://doi.org/10.1016/j.pmatsci.2023.101089

LINDNER, Sven; MASSNER, Alexander; GÄRTNER, Uwe; KOCH, Thomas. Impact of engine combustion on the reactivity of diesel soot from commercial vehicle engines. *International Journal of Engine Research,* v. 16, n. 1, p. 104-111, 2015. DOI: https://doi.org/10.1177/1468087414563360

LIU, Haifeng; LEE, Chia-Fon F.; HUO, Ming; YAO, Mingfa. Combustion characteristics and soot distributions of neat butanol and neat soybean biodiesel. *Energy & Fuels,* v. 25, n. 7, p. 3192-3203, 2011. DOI: https://doi.org/10.1021/ef1017412

MALARD, L. M.; PIMENTA, M. A.; DRESSELHAUS, G.; DRESSELHAUS, M. S. Raman spectroscopy in graphene. *Physics Reports,* 2009. DOI: https://doi.org/10.1016/j.physrep.2009.02.003

MATHER, T. A.; HARRISON, R. G.; TSANEV, V. I.; PYLE, D. M.; KARUMUDI, M. L.; BENNETT, A. J.; SAWYER, G. M.; HIGHWOOD, E. J. Observations of the plume generated by the December 2005 oil depot explosions and prolonged fire at Buncefield (Hertfordshire, UK) and associated atmospheric changes. *Proceedings of the Royal Society A*: Mathematical, Physical and Engineering Sciences, v. 463, n. 2081, p. 1153–1177, 2007. DOI: https://doi.org/10.1098/rspa.2006.1810

MINUTOLO, P.; RUSCIANO, G.; SGRO, L. A.; PESCE, G.; SASSO, A.; D'ANNA, A. Surface enhanced Raman spectroscopy (SERS) of particles produced in premixed flame across soot threshold. *Proceedings of the Combustion Institute,* v. 33, n. 1, p. 649-657, 2011. DOI: https://doi.org/10.1016/j.proci.2010.07.077

MIRANDA, Alisson M.; CASTILHO-ALMEIDA, Eduardo W.; MARTINS FERREIRA, Erlon H.; MOREIRA, Gabriela F.; ACHETE, Carlos A.; ARMOND, Raigna A. S. Z.; DOS SANTOS, Helio F.; JORIO, Ado. Line shape analysis of the Raman spectra from pure and mixed biofuels esters compounds. *Fuel,* v. 115, p. 118-125, 2014. DOI: https://doi.org/10.1016/j.fuel.2013.06.038

PATEL, Mihir; AZANZA RICARDO, Cristy Leonor; SCARDI, Paolo; ASWATH, Pranesh B. Morphology, structure and chemistry of extracted diesel soot - Part I: transmission electron microscopy, Raman spectroscopy, X-ray photoelectron spectroscopy and synchrotron X-ray diffraction study. *Tribology International,* v. 52, p. 29-39, 2012. DOI: https://doi.org/10.1016/j.triboint.2012.03.004

RUSSO, Carmela; CIAJOLO, Anna. Effect of the flame environment on soot nanostructure inferred by Raman

spectroscopy at different excitation wavelengths. *Combustion and Flame,* v. 162, n. 6, p. 2431-2441, 2015. DOI: https://doi.org/10.1016/j.combustflame.2015.02.011

SADEZKY, A.; MUCKENHUBER, H.; GROTHE, H.; NIESSNER, R.; PÖSCHL, U. Raman microspectroscopy of soot and related carbonaceous materials: spectral analysis and structural information. *Carbon,* v. 43, n. 8, p. 1731-1742, 2005. DOI: https://doi.org/10.1016/j.carbon.2005.02.018

SEONG, Hee Je; BOEHMAN, André L. Evaluation of Raman parameters using visible Raman microscopy for soot oxidative reactivity. *Energy & Fuels,* v. 27, n. 3, p. 1613-1624, 2013. DOI: https://doi.org/10.1021/ef301520y

SHENG, Changdong. Char structure characterized by Raman spectroscopy and its correlations with combustion reactivity. *Fuel,* v. 86, n. 15, p. 2316-2324, 2007. DOI: https://doi.org/10.1016/j.fuel.2007.01.029

SHIHONG YAN; YI-JIN JIANG; NATHAN D. MARSH; ERIC G. EDDINGS; ADEL F. SAROFIM; RONALD J. PUGMIRE. *Study of the evolution of soot from various fuels.* 2005. DOI: https://doi.org/10.1021/ef049742u

SILVA, J. A. D.; SILVA, L. P. D.; CAMPOS, J. C. C.; SIQUEIRA, A. M. D. O.; GURGEL, A.; GÓMEZ, L. C. Dynamic mesh analysis by numerical simulation of internal combustion engines. *REM - International Engineering Journal,* 77, p. 27-37, 2023. DOI: https://doi.org/10.1590/0370-44672023770003

VANDER WAL, Randy L.; TOMASEK, Aaron J. Soot nanostructure: dependence upon synthesis conditions. *Combustion and Flame,* v. 136, n. 1-2, p. 129-140, 2004. DOI: https://doi.org/10.1016/j.combustflame.2003.09.008

VANDER WAL, Randy L.; YEZERETS, Aleksey; CURRIER, Neal W.; KIM, Do Heui; WANG, Chong Min. HRTEM study of diesel soot collected from diesel particulate filters. *Carbon,* v. 45, n. 1, p. 70-77, 2007. DOI: https://doi.org/10.1016/j.carbon.2006.08.005

WANG, Xiangang; CHEUNG, C. S.; DI, Yage; HUANG, Zuohua. Diesel engine gaseous and particle emissions fueled with diesel-oxygenate blends. *Fuel,* v. 94, n. 94, p. 317-323, 2012. DOI: https://doi.org/10.1016/j.fuel.2011.09.016

XIAO, Maoyu; LIU, Haifeng; BI, Xiaojie; WANG, Hu; LEE, Chia-fon F. Experimental and Numerical Investigation on Soot Behavior of Soybean Biodiesel under Ambient Oxygen Dilution in Conventional and Low-Temperature Flames. *Energy & Fuels,* v. 28, n. 4, p. 2663–2676, 2014. DOI: https://doi.org/10.1021/ef5002315

YILMAZ, Nadir; DAVIS, Stephen M. Formation of polycyclic aromatic hydrocarbons and regulated emissions from biodiesel and n-butanol blends containing water. *Journal of Hazardous Materials,* v. 437, 2022. DOI: https://doi.org/10.1016/j.jhazmat.2022.129360

YILMAZ, Nadir; DONALDSON, Burl. Combined effects of engine characteristics and fuel aromatic content on polycyclic aromatic hydrocarbons and toxicity. *Energy Sources, Part A*: recovery, utilization and environmental effects, v. 44, n. 4, p. 9156-9171, 2022. DOI: https://doi.org/10.1080/15567036.2022.2129880

YILMAZ, Nadir; RAFIEI, Milad; DONALDSON, Burl. Effect of diesel and pentanol blends on PAH formation and regulated pollutants. *Biofuels,* v. 14, n. 3, p. 293-301, 2023. DOI: https://doi.org/10.1080/17597269.2022.2134640

YILMAZ, Nadir; VIGIL, Francisco; DONALDSON, Burl. Effect of n-butanol addition to diesel fuel on reduction of PAH formation and regulated pollutants. *Polycyclic Aromatic Compounds,* 2022. DOI: https://doi.org/10.1080/10406638.2022.2153881

YILMAZ, Nadir; VIGIL, Francisco; DONALDSON, Burl. Effect of diesel and propanol blends on regulated pollutants and polycyclic aromatic hydrocarbons under lean combustion conditions. Environmental Progress and Sustainable *Energy,* v. 42, n. 2, 2023. DOI: https://doi.org/10.1002/ep.14020

YILMAZ, Nadir; VIGIL, Francisco M.; ATMANLI, Alpaslan; DONALDSON, Burl. Influence of fuel oxygenation on regulated pollutants and unregulated aromatic compounds with biodiesel and n-pentanol blends. *International Journal of Energy Research,* v. 2023, p. 1-11, 2023. DOI: https://doi.org/10.1155/2023/3040073

YOON, Seung Hyun; SUH, Hyun Kyu; LEE, Chang Sik. Effect of Spray and EGR Rate on the Combustion and Emission Characteristics of Biodiesel Fuel in a Compression Ignition Engine. *Energy & Fuels,* v. 23, n. 3, p. 1486–1493, 2009. DOI: https://doi.org/10.1021/ef800949a

ZAIDA, Alon; BAR-ZIV, Ezra; RADOVIC, Ljubisa R.; LEE, Young-Jae. Further development of Raman Microprobe spectroscopy for characterization of char reactivity. *Proceedings of the Combustion Institute,* v. 31, n. 2, p. 1881-1887, 2007. DOI: https://doi.org/10.1016/j.proci.2006.07.011